EUROPEAN FUSION DEVELOPMENT AGREEMENT

EFDA–JET–CP(03)01-38

J.-S. Lönnroth, V.V. Parail, G. Corrigan, C. Figarella, X. Garbet, D. Heading,
G.T.A. Huysmans, A. Loarte, G. Saibene, R.R.E. Salomaa, R. Sartori,
S. Sharapov, J. Spence and JET EFDA Contributors

Predictive Transport Modelling with Theory-Based and Semi-Empirical Models for Different ELMy H-Mode scenarios

Predictive Transport Modelling with Theory-Based and Semi-Empirical Models for Different ELMy H-Mode scenarios

J.-S. Lönnroth[1], V.V. Parail[2], G. Corrigan[2], C. Figarella[3], X. Garbet[3], D. Heading[2], G.T.A. Huysmans[3], A. Loarte[4], G. Saibene[4], R.R.E. Salomaa[2], R. Sartori[4], S. Sharapov[2], J. Spence[2] and JET EFDA Contributor*

[1]Association EURATOM-Tekes, Helsinki University of Technology, Finland
[2]EURATOM/UKAEA Fusion Association, Culham Science Centre, United Kingdom
3Association EURATOM-CEA, CEA Cadarache, France
4EFDA Close Support Unit, c/o MPI für Plasmaphysik, Garching, Germany
**See Annex of J. Pamela et al., "Overview of Recent JET Results and Future Perspectives", Fusion Energy 2000 (Proc. 18th Int. Conf. Sorrento, 2000), IAEA, Vienna (2001).*

Preprint of Paper to be submitted for publication in Proceedings of the
EPS Conference on Controlled Fusion and Plasma Physics,
(St. Petersburg, Russia, 7-11 July 2003)

INTRODUCTION

It is well known that H-mode plasmas can exhibit several different types of Edge Localized Modes (ELMs). Type I or "giant" ELMs are the most commonly observed type of ELMs in plasmas with large enough heating power. They are large events capable of removing up to 10% of the plasma energy with a repetition frequency that increases with increased radial power flux across the last closed flux surface. Type III ELMs, which are small and frequent, remove of the order of 1% of the thermal energy content per ELM and are often seen slightly above the H-mode threshold power. Type III ELMs are characterized by an ELM frequency that decreases with power. Type II ELMs resemble type III ELMs, but are generally even tinier and more frequent. The distinction between types II and III is based on their different effects on plasma performance. Type II ELMs often occur in a mixed type I-II ELMy H-mode, i.e. a mode of operation with quasi-continuous type II ELMs interrupted by occasional large type I ELMs. This paper will focus on the modelling of plasmas with type II ELMs.

Pure type II ELMy H-modes and / or mixed type I-II ELMy H-modes have been observed in several different situations. The perhaps best example is the occurrence of type II ELMs in discharges with moderately strong gas puffing (e.g. about 5×10^{22} s^{-1} at JET). An increase in the level of external neutral gas puffing can trigger a transition from pure type I ELMy H-mode to mixed type I-II ELMy H-mode and eventually to pure type III ELMy H-mode [1]. Strong gas puffing leads to high edge density, which seems to be a common feature also in other scenarios with type II ELMs. High poloidal beta β_p, where b is the ratio of the total pressure to the magnetic pressure, is another effect generally favourable for the occurrence of type II ELMs. In the case of JT-60U, $\beta_p > 1.7$ seems to be necessary for type II ELMs to occur [2]. Pure type II as well mixed type I-II ELMy H-modes have also been found to occur frequently in JT-60U discharges with high safety factor q at the edge and high triangularity δ [3, 4]. Furthermore, plasmas with pure type II or mixed type I-II ELMs have frequently been observed in ASDEX Upgrade in quasi double null discharges, i.e. in discharges with a magnetic configuration with a second X-point in the proximity of the plasma. Type II ELMs in quasi double null configurations have been reported for high densities and a broad range of triangularities and edge safety factors.

1. ELM MODEL

It is assumed that the ELMs are triggered by ballooning mode instabilities controlled mainly by the pressure gradient. Different ELM types are defined according to changes in ballooning stability. Figure 1 contains three different MHD stability diagrams in α-σ space corresponding to situations with type I, mixed type I-II and type III ELMy H-mode. The stability diagrams have been obtained by running the MHD stability codes HELENA and MISHKA [6] on the output of simulations with the 1.5D transport code JETTO [7] for three different levels of gas puffing and thus for three different densities. The diagrams show the mode numbers of the most unstable kink, peeling or ballooning modes (with $n < 15$) at a number of locations in the α-s space as well as the ideal $n = \infty$ ballooning

unstable region. The operational point has been plotted for the magnetic surfaces $\rho = 0.91$ (inside the ETB), $\rho = 0.95$ (near the top of the ETB) and $\rho = 0.99$ (near the separatrix).

The stability diagram in frame fig.1(a) is for the lowest density (no external gas puffing). In this case the whole pedestal is second stable. Stability is determined by the finite *n* stability limit at $a \approx 6$ throughout the pedestal. In the present model, this situation corresponds to a pure type I ELMy H-mode.

Frame fig.1(b) is for an intermediate density (gas puffing $G = 4\times10^{22}$ s^{-1}). In this case, most of the pedestal is still second stable, but the outermost edge is infinite *n* ballooning unstable due to a strong increase in magnetic shear, a situation resulting in type II ELMs. Stability at the edge is effectively determined by the first ballooning stability limit at $a \approx 3$, whereas the finite *n* stability limit at $a \approx 6$ still holds for the inner parts of the pedestal. The situation thus corresponds to a mixed type I-II ELMy H-mode.

The stability diagram in frame fig.1(c) has been obtained for a very high density (gas puffing $G = 1\times10^{23}$ s^{-1}). In this case magnetic shear is so strong that the whole pedestal is infinite *n* ballooning unstable, so that stability throughout the pedestal is determined by the first stability limit at $a \approx 3$. In the present model, this situation corresponds to a pure type III ELMy H-mode.

In particular, the model explains the experimentally observed transition from type I to type III ELMy H-mode with increasing gas puffing as well as the accompanying increase in ELM frequency and deterioration of plasma confinement as a transition from second to first ballooning stability. According to the model, the high ELM frequencies in type II and type III ELMy H-mode with respect to type I ELMy H-mode are due to a decrease in the inherent critical pressure gradient. For type III ELMs, the deterioration in plasma confinement occurs, because the ELMs reshape the pedestal pressure profile, which results in lower pedestal temperature and thus lower core temperature due to profile stiffness.

Since modelling of mixed type I-II ELMy H-mode requires separate stability limits for the outermost and the inner regions of the pedestal, the ETB has been divided into two regions in JETTO. In the inner region, the critical pressure gradient is set at the value defined by the finite *n* stability limit, typically $\alpha \approx 6$, whereas in the outer region it is set at the value defined by the first stability limit, typically $\alpha \approx 3$. Depending on which of the two stability criteria is violated, different Gaussian-shaped perturbations are applied to the radial profiles of the transport coefficients in the pedestal region, as shown in Fig.2. The inner region ELMs with wide large-amplitude perturbations corresponding to type I ELMs, whereas the outer region triggers narrow small-amplitude perturbations corresponding to type II ELMs. The use of Gaussian-shaped ELMs is motivated by the fact that the eigenfunctions of the MHD modes supposed to be driving the ELMs have Gaussian shapes in linear theory.

Numerical studies with MISHKA support the understanding that the infinite *n* ballooning modes assumed to drive the type II ELMs are very edge localized. The analysis shows that ballooning modes become very narrow and edge localized in the high *n* limit, if a significant part of the pedestal

is second stable and only the outermost edge is infinte *n* ballooning unstable. Figure 3 illustrates the result for $n = 40$. By perturbing the edge current, the part of the pedestal being second stable has been varied. Frame (a) shows the eigenfunction for a situation with the edge unstable from $\psi = 0.935$ to $\psi = 1.000$. The width of the eigenfunction is comparable to the width of the pedestal. In frame (b), the pedestal is unstable only from $y = 0.990$ to $y = 1.000$. In this case, the eigenfunction is almost as narrow as the unstable region and centred close to the edge of the plasma.

2. SIMULATION RESULTS

JETTO simulations with the new ELM model reproduce the experimental dynamics of mixed type I-II ELMy H-mode. Frame (a) in Fig.4 shows the ion thermal conductivity as a function of time in a typical simulation with small frequent type II ELMs interrupted by occasional large type I ELMs. In frame (b) in Fig.4, the plasma thermal energy content of the simulation of mixed type I-II ELMy H-mode has been compared with reference simulations for pure type I and pure type III ELMy H-mode. Type I and type III ELMy H-modes are simulated by using only a single Gaussian-shaped perturbation covering the whole pedestal. Frame (b) in Fig.4 shows that according to the simulations, plasma confinement in mixed type I-II ELMy H-mode is much better than in pure type III ELMy H-mode, which is consistent with experimental observations. Compared to pure type I ELMy H-mode confinement is slightly lower, as observed especially at ASDEX Upgrade [5].

It the context of introducing the new ELM model it was already shown that strong gas puffing and high edge density are favourable for mixed type I-II ELMy H-mode. Next, the effect of β_p, edge safety factor, triangularity and magnetic configuration will be investigated.

Figure 5 shows MHD stability diagrams for the magnetic surfaces $\rho = 0.97$ and $\rho = 0.99$ for two predictive JETTO simulations differing only with respect to β_p. At the time of the analysis, $\beta_p = 1.129$ in the low β_p simulation and $\beta_p = 1.155$ in the high β_p run. From Fig.5 it can be inferred that the whole pedestal is second stable in the case with low β_p. In the high β_p case, the system still enters second stability, but becomes infinite *n* ballooning unstable at the very edge, as illustrated by the frame for $\rho = 0.99$. In the present model, this means that the low β_p case corresponds to a pure type I ELMy H-mode, whereas the high b_p case represents a mixed type I-II ELMy H-mode. This implies that high β_p is favourable for mixed type I-II ELMy H-mode according to the simulations.

Similarly, Fig.6 compares two predictive JETTO simulations with different edge safety factors, $q = 4.33$ and $q = 5.51$ at the separatrix. In the simulation with low q, the whole pedestal is second stable, whereas with high q, the system still enters second stability, but the very edge is infinite *n* ballooning unstable. Again, the former case corresponds to type I ELMy H-mode and the latter one to mixed type I-II ELMy H-mode, which implies that a high edge safety factor is favourable for type II ELMs.

A similar comparison has been made for predictive JETTO simulations with different triangularities. The obtained results indicate that high triangularity is not necessarily favourable for type II ELMs. Experimentally, type II ELMs have been obtained for combinations of high edge safety factor and high triangularity. This result indicates that the edge safety factor is actually the more important of the two quantities with respect to favourability for type II ELMs.

In a series of simulations, the effect of a quasi double null magnetic configuration versus a single null configuration on favourability for type II ELMs has been investigated. Somewhat different results have been obtained with different equilibria, but the general trend seems to be that quasi double null configurations are more infinite *n* ballooning unstable at the edge than single null configurations and thus more favourable for type II ELMs.

SUMMARY

A new model for various ELM types has been presented. In particular, this model can reproduce the experimental dynamics of mixed type I-II ELMy H-mode in simulations with JETTO. It has been shown that certain scenarios such as strong gas puffing, high β_p and high edge safety factor are favourable for type II ELMs.

[1]. G. Saibene *et al*., Proc. 28th EPS Conference, Madeira, 18-22 June 2001.
[2]. Y. Kamada *et al*., Plasma Phys. Control. Fusion **44** A279 (2002).
[3]. Y. Kamada *et al*., Plasma Phys. Control. Fusion **42** A247 (2000).
[4]. L. Lao et al., Nucl. Fusion **41** 295 (2001).
[5]. J. Stober *et al*., Nucl. Fusion **41** 1123 (2001).
[6]. A.B. Mikhailovskii *et al*., Plasma Phys. Rep. **23** 844 (1997).
[7]. G. Cennachi, A. Taroni, JET-IR(88)03 (1988).

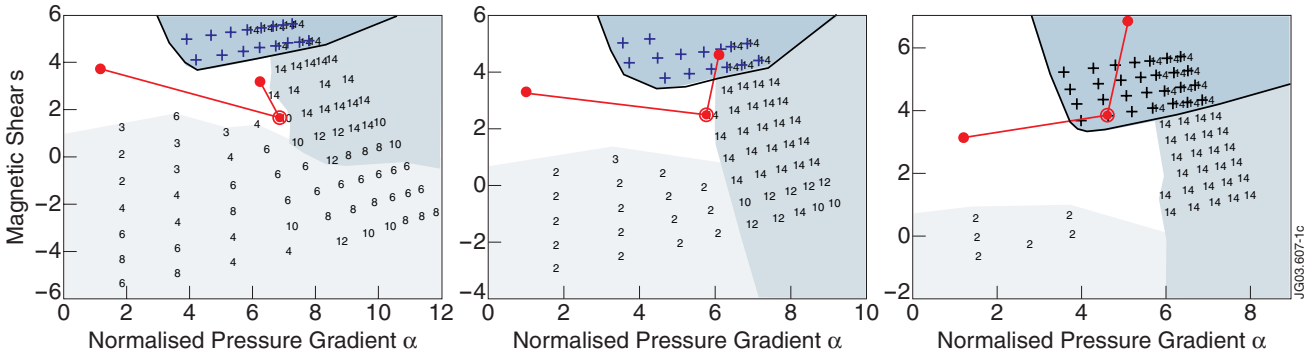

Figure 1: MHD stability diagrams for JETTO simulations with different levels of external neutral gas puffing: $\Gamma = 0$, $\Gamma = 4\times10^{22}\ s^{-1}$ and $\Gamma = 1\times10^{23}\ s^{-1}$. The numbers indicate the mode number of the most unstable finite n mode. The n = ∞ ballooning unstable region has been marked with crosses. The operational point has been plotted for $\rho = 0.92$ 0.95 and 0.99. The location of the top of the ETB at $\rho = 0.95$ has been marked with a circle.

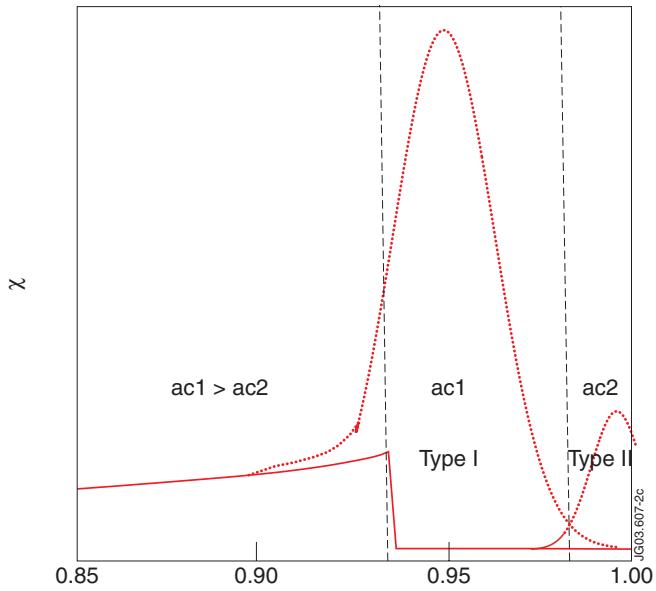

Figure 2: Schematic picture of the perturbations to the radial profiles of the transport coefficients induced by type I and type II ELMs in the JETTO implementation of the new ELM model.

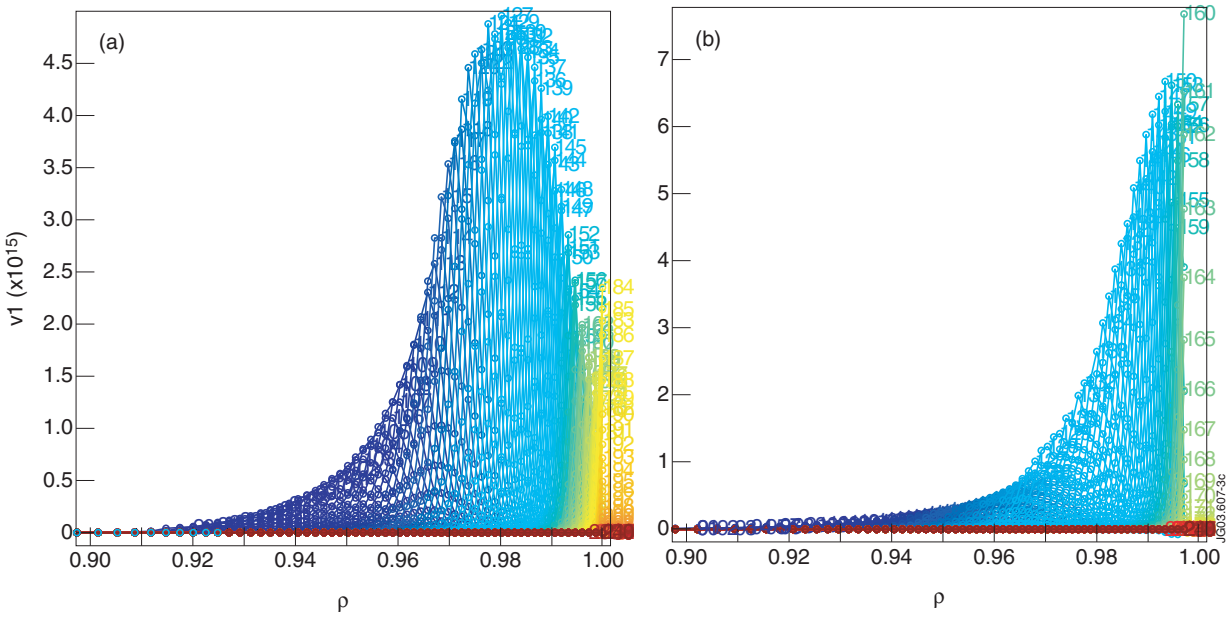

Figure 3: Eigenfunctions of n = 40 ballooning modes in situations with the edge of the pedestal n = ∞ ballooning unstable and the inner part of it second ballooning stable. (a) The edge unstable from ψ = 0.935 to ψ = 1.000, i.e. most of the pedestal unstable. (b) The edge unstable from ψ = 0.990 to ψ = 1.000.

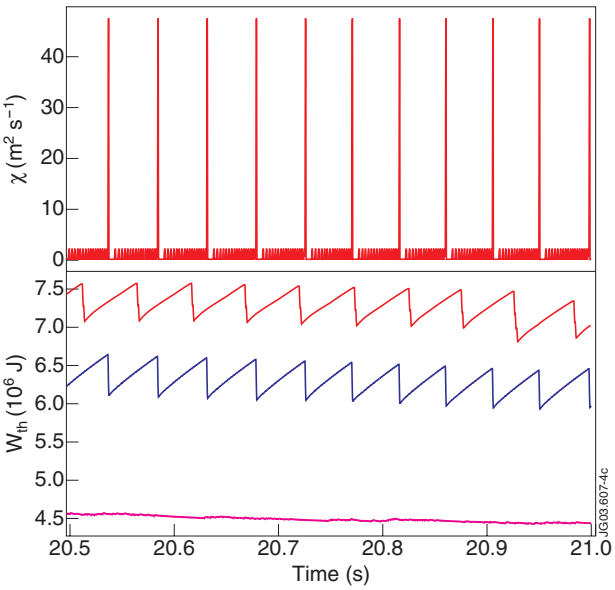

Figure 4.:(a) Ion thermal concuctivity as a function of time in a typical simulation of mixed type I-II ELMy H-mode. (b) Plasma thermal energy content as a function of time in a reference simulation for pure type I ELMy H-mode (red curve), in the simulation of mixed type I-II ELMy H-mode (blue curve) and in a reference simulation of pure type III ELMy H-mode (magenta curve).

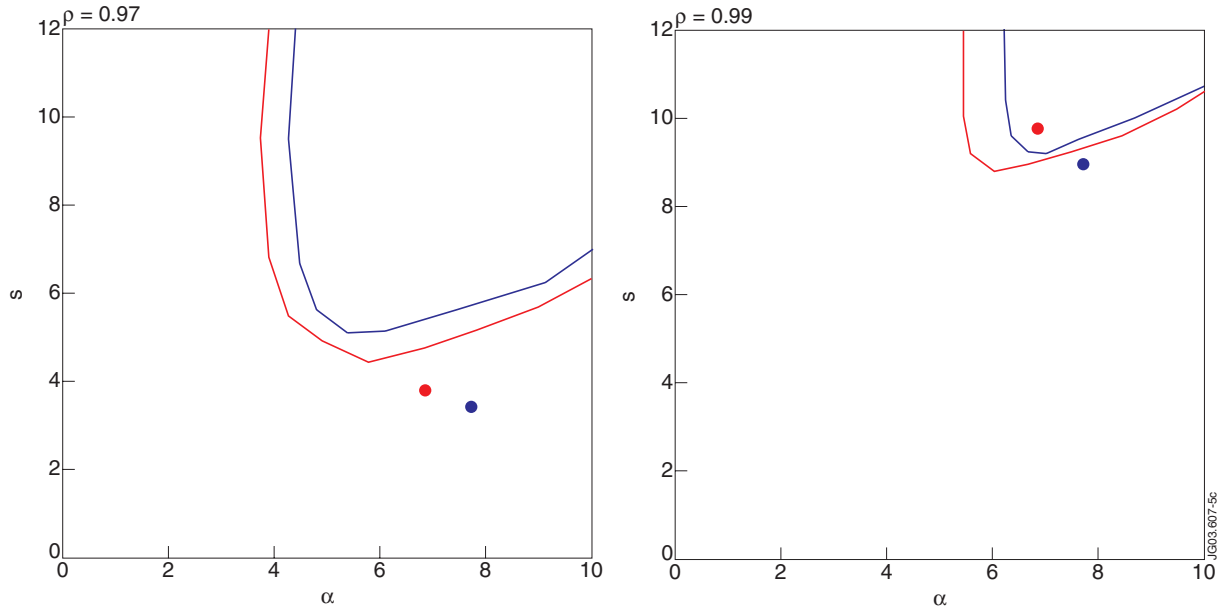

Figure 5. Infinite n ballooning stability diagrams for flux surfaces $\rho = 0.97$ and $\beta = 0.99$ for two predictive JETTO simulations with $\beta_p = 1.129$ (in blue) and $\beta_p = 1.155$ (in red).

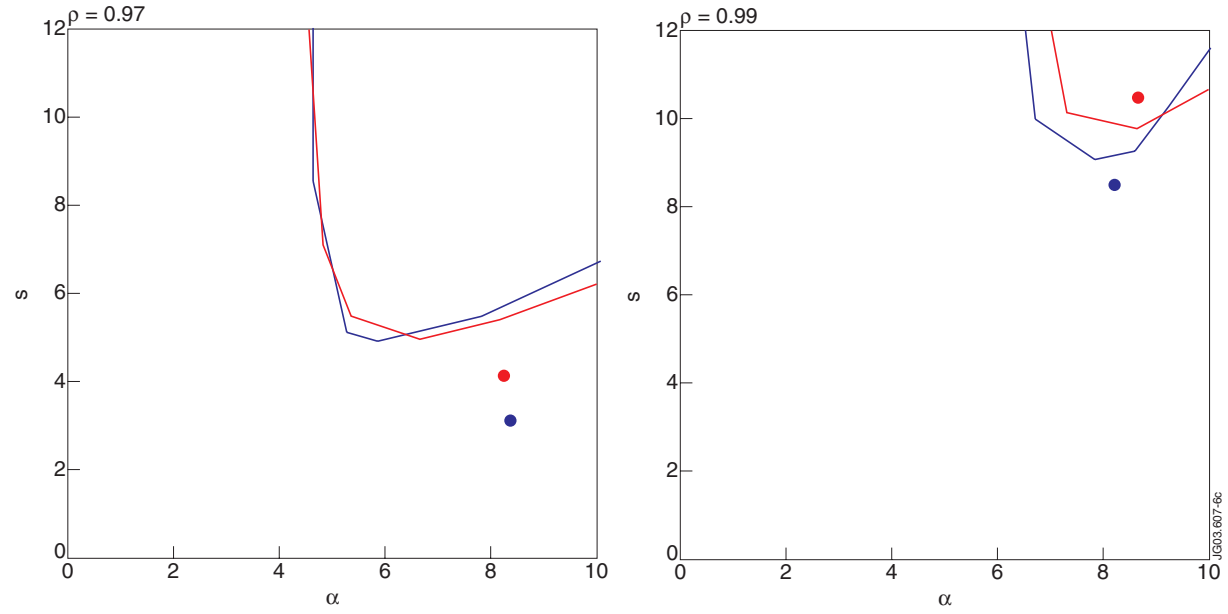

Figure 6: Infinite n ballooning stability diagrams for flux surfaces $\rho = 0.97$ and $\rho = 0.99$ for two predictive JETTO simulations with $q = 4.33$ (in blue) and $q = 5.51$ (in red) at the separatrix.